

**$\beta$  decay of semi-magic  $^{130}\text{Cd}$ : Revision and extension of the level scheme of  $^{130}\text{In}$** 

A. Jungclauss,<sup>1</sup> H. Grawe,<sup>2</sup> S. Nishimura,<sup>3</sup> P. Doornenbal,<sup>3</sup> G. Lorusso,<sup>3,4,5</sup> G. S. Simpson,<sup>6</sup> P.-A. Söderström,<sup>3</sup> T. Sumikama,<sup>7</sup> J. Taprogge,<sup>1,8,3</sup> Z. Y. Xu,<sup>9</sup> H. Baba,<sup>3</sup> F. Browne,<sup>10,3</sup> N. Fukuda,<sup>3</sup> R. Gernhäuser,<sup>11</sup> G. Gey,<sup>6,12,3</sup> N. Inabe,<sup>3</sup> T. Isobe,<sup>3</sup> H. S. Jung,<sup>13,\*</sup> D. Kameda,<sup>3</sup> G. D. Kim,<sup>14</sup> Y.-K. Kim,<sup>14,15</sup> I. Kojouharov,<sup>2</sup> T. Kubo,<sup>3</sup> N. Kurz,<sup>2</sup> Y. K. Kwon,<sup>14</sup> Z. Li,<sup>16</sup> H. Sakurai,<sup>3,9</sup> H. Schaffner,<sup>2</sup> Y. Shimizu,<sup>3</sup> K. Steiger,<sup>11</sup> H. Suzuki,<sup>3</sup> H. Takeda,<sup>3</sup> Zs. Vajta,<sup>17,3</sup> H. Watanabe,<sup>3</sup> J. Wu,<sup>16,3</sup> A. Yagi,<sup>18</sup> K. Yoshinaga,<sup>19</sup> G. Benzoni,<sup>20</sup> S. Bönig,<sup>21</sup> K. Y. Chae,<sup>22</sup> L. Coraggio,<sup>23</sup> J.-M. Daugas,<sup>24</sup> F. Drouet,<sup>6</sup> A. Gadea,<sup>25</sup> A. Gargano,<sup>23</sup> S. Ilieva,<sup>21</sup> N. Itaco,<sup>23,26</sup> F. G. Kondev,<sup>27</sup> T. Kröll,<sup>21</sup> G. J. Lane,<sup>28</sup> A. Montaner-Pizá,<sup>25</sup> K. Moschner,<sup>29</sup> D. Mücher,<sup>11</sup> F. Naqvi,<sup>30</sup> M. Niikura,<sup>9</sup> H. Nishibata,<sup>18</sup> A. Odahara,<sup>18</sup> R. Orlandi,<sup>31,32</sup> Z. Patel,<sup>5</sup> Zs. Podolyák,<sup>5</sup> and A. Wendt<sup>29</sup>

<sup>1</sup>*Instituto de Estructura de la Materia, CSIC, E-28006 Madrid, Spain*

<sup>2</sup>*GSI Helmholtzzentrum für Schwerionenforschung GmbH, 64291 Darmstadt, Germany*

<sup>3</sup>*RIKEN Nishina Center, RIKEN, 2-1 Hirosawa, Wako-shi, Saitama 351-0198, Japan*

<sup>4</sup>*National Physical Laboratory, NPL, Teddington, Middlesex TW11 0LW, United Kingdom*

<sup>5</sup>*Department of Physics, University of Surrey, Guildford GU2 7XH, United Kingdom*

<sup>6</sup>*LPSC, Université Joseph Fourier Grenoble 1, CNRS/IN2P3, Institut National Polytechnique de Grenoble, F-38026 Grenoble Cedex, France*

<sup>7</sup>*Department of Physics, Tohoku University, Aoba, Sendai, Miyagi 980-8578, Japan*

<sup>8</sup>*Departamento de Física Teórica, Universidad Autónoma de Madrid, E-28049 Madrid, Spain*

<sup>9</sup>*Department of Physics, University of Tokyo, Hongo 7-3-1, Bunkyo-ku, 113-0033 Tokyo, Japan*

<sup>10</sup>*School of Computing, Engineering and Mathematics, University of Brighton, Brighton BN2 4GJ, United Kingdom*

<sup>11</sup>*Physik Department E12, Technische Universität München, D-85748 Garching, Germany*

<sup>12</sup>*Institut Laue-Langevin, B.P. 156, F-38042 Grenoble Cedex 9, France*

<sup>13</sup>*Department of Physics, Chung-Ang University, Seoul 156-756, Republic of Korea*

<sup>14</sup>*Rare Isotope Science Project, Institute for Basic Science, Daejeon 305-811, Republic of Korea*

<sup>15</sup>*Department of Nuclear Engineering, Hanyang University, Seoul 133-791, Republic of Korea*

<sup>16</sup>*School of Physics and State key Laboratory of Nuclear Physics and Technology, Peking University, Beijing 100871, China*

<sup>17</sup>*MTA Atomki, P.O. Box 51, Debrecen H-4001, Hungary*

<sup>18</sup>*Department of Physics, Osaka University, Machikaneyama-machi 1-1, Osaka 560-0043 Toyonaka, Japan*

<sup>19</sup>*Department of Physics, Faculty of Science and Technology, Tokyo University of Science, 2641 Yamazaki, Noda, Chiba, Japan*

<sup>20</sup>*INFN, Sezione di Milano, via Celoria 16, I-20133 Milano, Italy*

<sup>21</sup>*Institut für Kernphysik, Technische Universität Darmstadt, D-64289 Darmstadt, Germany*

<sup>22</sup>*Department of Physics, Sungkyunkwan University, Suwon 440-746, Republic of Korea*

<sup>23</sup>*Istituto Nazionale di Fisica Nucleare, Complesso Universitario di Monte S. Angelo, I-80126 Napoli, Italy*

<sup>24</sup>*CEA, DAM, DIF, 91297 Arpajon cedex, France*

<sup>25</sup>*Instituto de Física Corpuscular, CSIC–University of Valencia, E-46980 Paterna, Spain*

<sup>26</sup>*Seconda Università di Napoli, Dipartimento di Matematica e Fisica, 2-81100 Caserta, Italy*

<sup>27</sup>*Nuclear Engineering Division, Argonne National Laboratory, Argonne, Illinois 60439, USA*

<sup>28</sup>*Department of Nuclear Physics, Research School of Physical Sciences and Engineering, Australian National University, Canberra, A.C.T 0200, Australia*

<sup>29</sup>*IKP, University of Cologne, D-50937 Cologne, Germany*

<sup>30</sup>*Wright Nuclear Structure Laboratory, Yale University, New Haven, Connecticut 06520-8120, USA*

<sup>31</sup>*Instituut voor Kern- en Stralingsfysica, K.U. Leuven, B-3001 Heverlee, Belgium*

<sup>32</sup>*Advanced Science Research Center, Japan Atomic Energy Agency, Tokai, Ibaraki, 319-1195, Japan*

(Received 9 June 2016; published 1 August 2016)

The  $\beta$  decay of the semi-magic nucleus  $^{130}\text{Cd}$  has been studied at the RIBF facility at the RIKEN Nishina Center. The high statistics of the present experiment allowed for a revision of the established level scheme of  $^{130}\text{In}$  and the observation of additional  $\beta$  feeding to high-lying core-excited states in  $^{130}\text{In}$ . The experimental results are compared to shell-model calculations employing a model space consisting of the full major  $N = 50$ – $82$  neutron and  $Z = 28$ – $50$  proton shells and the NA-14 interaction, and good agreement is found.

DOI: [10.1103/PhysRevC.94.024303](https://doi.org/10.1103/PhysRevC.94.024303)

**I. INTRODUCTION**

The  $\beta$ -decay properties of the classical  $N = 82$  waiting-point nucleus  $^{130}\text{Cd}$  play an important role in astrophysical  $r$ -process calculations. Its half-life, which directly influences the amplitude and shape of the second abundance peak around

\*Present address: Department of Physics, University of Notre Dame, Notre Dame, Indiana 46556, USA.

$A = 130$ , was measured several times over the last three decades. The first measurement, presented by Kratz *et al.* in 1986, employed the analysis of  $\beta$ -delayed neutron decay curves at ISOLDE and yielded a value of  $T_{1/2} = 195(35)$  ms [1]. In 2011 the same group reported the more precise value of  $T_{1/2} = 162(7)$  ms [2] obtained using the same technique. In 2015 a much shorter half-life of  $T_{1/2} = 127(2)$  ms was reported from an experiment performed at RIKEN in which the observation of the decay events in coincidence with  $\gamma$  transitions in the daughter nucleus  $^{130}\text{In}$  allowed for an unequivocal ion identification [3]. Very recently this half-life was confirmed by a measurement performed with the GRIFFIN spectrometer at TRIUMF in which a value of  $T_{1/2} = 126(4)$  ms was deduced [4].

As was shown in Ref. [5] the  $\beta$  decay of  $^{130}\text{Cd}$  is dominated by the  $\nu g_{7/2} \rightarrow \pi g_{9/2}$  Gamow-Teller transition to a  $1^+$  state at an excitation energy of 2120 keV, which occurs in about 70% of all decays. The shell-model calculations presented in Refs. [5,6] underestimated the energy of this  $\pi g_{9/2} \nu g_{7/2}^{-1}$  state by 550–750 keV. This discrepancy could only be solved by introducing empirical monopole modifications to the employed interaction [7]. The total  $\beta$ -feeding intensity quoted in Ref. [5] amounts to at most 84%, while the  $\beta$ -delayed neutron emission probability is  $P_n = 3.5(1.0)\%$  [2]. Consequently additional feeding to excited states in  $^{130}\text{In}$  must exist, and indeed a number of high-energy  $\gamma$  rays were already observed [8] in addition to the transitions reported in Ref. [5]. The aim of the present work was to search for the missing  $\beta$ -feeding intensity to highly excited  $1^+$  states and thus fix the position of core-excited states in the hole-hole nucleus  $^{130}\text{In}$ .

## II. EXPERIMENT

Radioactive  $^{130}\text{Cd}$  ions were produced via fission of a  $^{238}\text{U}$  beam with a kinetic energy of 345 MeV/ $u$  and an average intensity of 8–10 pA on a Be target at the Radioactive Isotope Beam Factory (RIBF) at RIKEN in the framework of the EURICA project [9,10]. The produced  $^{130}\text{Cd}$  ions were identified in-flight event by event by the BigRIPS separator [11] on the basis of measured energy loss,  $\Delta E$ , time of flight, TOF, and magnetic rigidity,  $B\rho$ . Details about the identification procedure can be found in Ref. [12]. Two different settings of BigRIPS were used: one optimized for the maximum transmission of  $^{136}\text{Sn}$  and the other one tuned to predominantly transmit  $^{128}\text{Pd}$ . In total about  $1.5 \times 10^6$   $^{130}\text{Cd}$  ions were identified, transported through the ZeroDegree spectrometer (ZDS), and finally implanted into the WAS3ABi (Wide-range Active Silicon Strip Stopper Array for  $\beta$  and ion detection) Si array positioned at the focal plane of the ZDS. The WAS3ABi detector [9,10] consists of eight closely packed double-sided silicon strip detectors (DSSSDs) with an area of  $60 \times 40$  mm<sup>2</sup>, a thickness of 1 mm, and a segmentation of 40 horizontal and 60 vertical strips each. All decay events detected in WAS3ABi were stored and correlated offline in space and time with the implanted ions. The  $\gamma$  rays emitted following the  $\beta$  decay of the radioactive nuclei were detected by the EURICA array, which comprises 84 germanium crystals (12 large-volume cluster detectors [13] from the former EUROBALL spectrometer

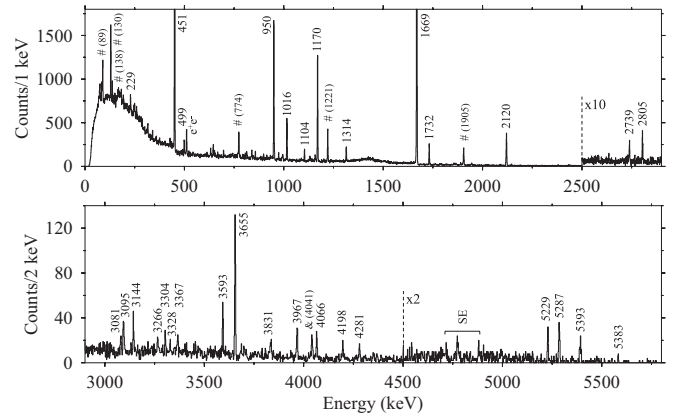


FIG. 1.  $\gamma$ -ray spectrum observed in prompt coincidence with the first  $\beta$  decay detected in WAS3ABi within 381 ms ( $=3T_{1/2}$ ) after the implantation of a  $^{130}\text{Cd}$  ion and requiring that the implantation and the decay occurred in the same DSSSD and with a maximum position difference of 1 mm in the horizontal and vertical directions. The most intense lines are labeled by their energies. Known transitions in  $^{130}\text{Sn}$ , populated following the  $^{130}\text{In}$  daughter decay, are labeled by a “#”, while the symbol “&” marks the most intense  $\gamma$  ray emitted in the decay of the strongest reaction channel  $^{132}\text{In}$  and falsely correlated to  $^{130}\text{Cd}$ . Single-escape peaks are labeled by SE.

[14]) arranged in a close geometry around the Si detectors. This geometry assures a high  $\gamma$ -ray detection efficiency of 8.5(4)% (2.9(3)%) for a  $\gamma$ -ray energy of 1 MeV (4 MeV) after applying appropriate add-back algorithms (summing the energies of neighboring crystals).

## III. DATA ANALYSIS AND RESULTS

Figure 1 shows the  $\gamma$ -ray spectrum observed in prompt coincidence with the first decay event after the implantation of a  $^{130}\text{Cd}$  ion in WAS3ABi. The time window between the implantation and the decay was limited to 381 ms, corresponding to three times the half-life of  $^{130}\text{Cd}$ ,  $T_{1/2} = 127(2)$  ms [3]. Only those events were considered in which the decay occurred in the same Si detector in which the ion was implanted, and the distance between implantation and decay in the two directions perpendicular to the beam axis was smaller than or equal to 1 mm. The two most intense lines in the spectrum are the ones with energies of 451 and 1669 keV which were assigned in Ref. [5] to form a cascade from an excited  $1^+$  state at an energy of 2120 keV via an intermediate level at 1669 keV (with a tentatively assigned spin of  $1^-$ ) to the  $1^-$  ground state. These two lines are truncated in Fig. 1 to allow for a better visibility of the many weaker transitions in the spectrum.  $\gamma$  rays emitted following the  $^{130}\text{In}$  daughter decay can easily be identified by comparing spectra sorted for different time intervals after the implantation. Furthermore, the  $^{130}\text{In} \rightarrow ^{130}\text{Sn}$  decay has already been studied in detail in the past [15] so that the energies of the strongest transitions are known. Contaminations due to chance correlations between  $\gamma$  rays, which are emitted in the decay of the nuclei which are implanted in highest quantities in the present experiment, and  $^{130}\text{Cd}$  nuclei on the other hand can

TABLE I. Energies and relative intensities, normalized to the most intense transition, of  $\gamma$  rays observed following the  $\beta$  decay of  $^{130}\text{Cd}$  in the present work and in Refs. [5,8].  $E_i$  and  $E_f$  are the initial and final state energies corresponding to the placement of the transitions in the level scheme of  $^{130}\text{In}$  (in parentheses in cases of tentative assignments). The errors quoted for the  $\gamma$ -ray energies reflect the uncertainties from the fit. The systematic uncertainties from the calibration can be estimated to 0.2, 0.6, and 1.0 keV for energies <1, in the range 1.0–3.5, and >3.5 MeV, respectively.

Present work				From Refs. [5,8]			
$E_\gamma$ (keV)	$I_\gamma^{\text{rel}}$	$E_i$ (keV)	$E_f$ (keV)	$E_\gamma$ (keV)	$I_\gamma^{\text{rel}}$	$E_i$ (keV)	$E_f$ (keV)
229.1(2)	16(3)	(4197)	(3967)				
388.4(2)	76(5)	388	0	388.7(5)	40(26)	388	0
450.9(2)	1000(51)	451	0	451.0(2)	886(36)	2120	1669
498.9(2)	14(2)	950	0				
950.0(2)	225(13)	950	0	949.9(5)	221(33)	2120	1170
1015.9(2)	69(8)	1016	0	1015.5(2) <sup>a</sup>	55(10)		
1104.1(2)	20(3)	2120	1016				
				1138.4(4) <sup>a</sup>	17(3)		
1170.1(2)	204(21)	2120	950	1170.3(3)	200(2)	1170	0
1314.3(2) <sup>a</sup>	29(4)			1314.4(2) <sup>a</sup>	25(2)		
1669.2(2)	998(101)	2120	451	1669.2(1)	1000	1669	0
1731.8(2)	53(6)	2120	388	1731.8(1)	44(4)	2120	1170
2120.3(2)	114(12)	2120	0	2120.1(5)	111(6)	2120	0
2582(1)	4(1)	3532	950	2585.5(9)	13(3)	2586	0
2739.0(3)	8(2)	3755	1016	2738.3(6)	13(3)	4407	1669
2804.5(2)	13(3)	3755	950	2804.9(3)	11(2)	5391	2586
3081.4(5)	5(2)	3532	451				
3094.1(4)	9(2)	4044	950				
3143.7(3)	11(3)	3532	388				
3265.5(7)	3(2)	3717	451				
3304.0(4)	5(2)	3755	451				
3328.4(5)	3(2)	3717	388				
3366.1(9)	5(2)	3755	388				
3593.1(2)	14(3)	4044	451				
3655.2(2)	42(6)	4044	388				
3831(1)	3(2)	4281	451				
3967.1(3)	12(2)	(3967)	(0)				
4065.9(4)	9(2)	(4066)	(0)				
4197.3(10)	8(3)	(4197)	(0)				
4281.0(4)	4(1)	4281	0				
				4407.0(10)	5(1)	4407	0
				4631.0(10)	6(1)	4631	0
				5098.0(10)	11(3)	5098	0
				5196.0(10)	7(2)	5196	0
5228.8(6)	7(2)	5229	0				
5285.4(5)	11(2)	5285	0				
5393.3(5)	8(2)	5393	0	5391.0(10)	4(2)	5391	0
5583(1)	2(1)	5583	0				

<sup>a</sup>Not placed in the level scheme.

be identified by investigating the intensity ratios of the lines in spectra sorted with different requirements with respect to the spatial correlation. The more strict these conditions are, the smaller the probability of random correlations will be. Applying these criteria, 33  $\gamma$  rays were assigned to follow the decay of  $^{130}\text{Cd}$  and their energies and relative intensities are listed in the first two columns of Table I. In Ref. [5], besides the 451–1669 keV cascade, two  $\gamma$ -ray sequences with energies of 950–1171 keV and 1732–389 keV, defining intermediate states at excitation energies of 1171 and 389 keV, respectively, as well as a ground state transition have been assigned to

depopulate the  $1^+$  state at 2120 keV. Note that the 389 keV  $\gamma$  ray has also been observed in in-flight fission studies [16,17] and assigned as an  $M2$  transition from a 389 keV state with spin  $3^+$  to the  $1^-$  ground state. The half-life of the  $3^+$  state was determined as  $T_{1/2} = 3.1(3) \mu\text{s}$  [17] and  $T_{1/2} = 1\text{--}10 \mu\text{s}$  [16], respectively. All the transitions mentioned above are also observed in the present work. From a fit to the time distribution of the 388 keV  $\gamma$  ray relative to the  $^{130}\text{Cd}$   $\beta$  decay, a half-life of  $T_{1/2} = 4.4(2) \mu\text{s}$  is obtained. In addition a 499 keV  $\gamma$  ray is visible in Fig. 1 which is found to be emitted in prompt coincidence with both the 451 and 1170 keV transitions, as

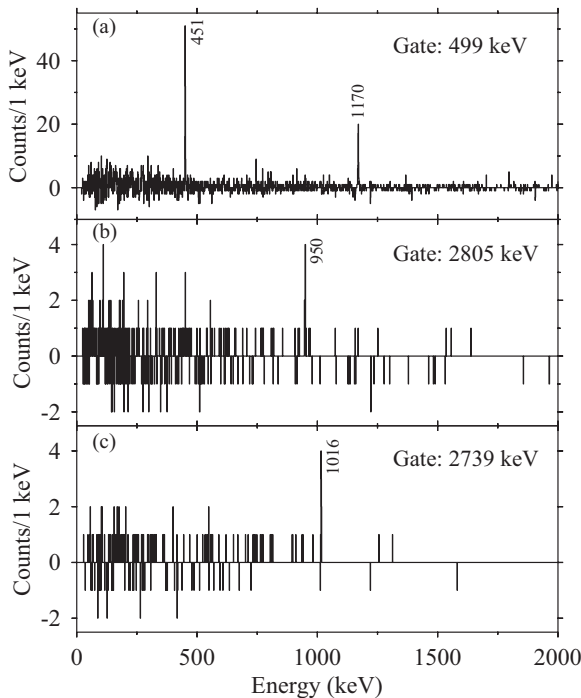


FIG. 2. Spectrum of  $\gamma$  rays observed in prompt coincidence with (a) the 499 keV, (b) the 2805 keV, and (c) the 2739 keV transition emitted following the first or second decay detected in WAS3ABi within 381 ms after the implantation of a  $^{130}\text{Cd}$  ion.

shown in Fig. 2(a). This observation suggests its placement parallel to the 950 keV transition. The 2805 keV  $\gamma$  ray, which in Ref. [8] has been assigned to decay from a state at 5391 keV to a 2586 keV level which in turn decays directly to the ground state [5], was observed in the present work in coincidence with the 950 keV transition [see Fig. 2(b)]. However, a placement of the 2805 keV on top of the 950 keV transition, i.e., feeding the 2120 keV level, would necessarily imply a clear coincidence relation with the 451 keV  $\gamma$  ray which is a much stronger decay branch of this state. The nonobservation of a coincidence between the 451 and the 2805 keV  $\gamma$  ray therefore strongly suggests an inversion of the order within the 950–1170 keV cascade in the decay of the 2120 keV state thus establishing a new level at 950 keV (and annulling the one established at an excitation energy of 1170 keV in Refs. [5,8]). This modification necessarily requires also the inversion of the 451–1669 keV cascade since the 451 and 499 keV transitions, placed parallel to the one with 950 keV, are observed in coincidence with the 1170 keV  $\gamma$  ray. As a consequence the excited state proposed at an excitation energy of 1669 keV in Refs. [5,8] is now replaced by one at an excitation energy of 451 keV. In Ref. [8] the observation of a 1016 keV  $\gamma$  ray was reported which, however, could not be placed in the level scheme. This transition is observed also in the present work and furthermore in coincidence with a 1104 keV  $\gamma$  ray. The fact that the sum of the two energies equals 2120 keV suggests that these two transitions form an additional cascade decaying from the 2120 keV level to the ground state. The much higher intensity of the 1016 keV  $\gamma$  ray suggests its placement as ground state transition. This assignment is

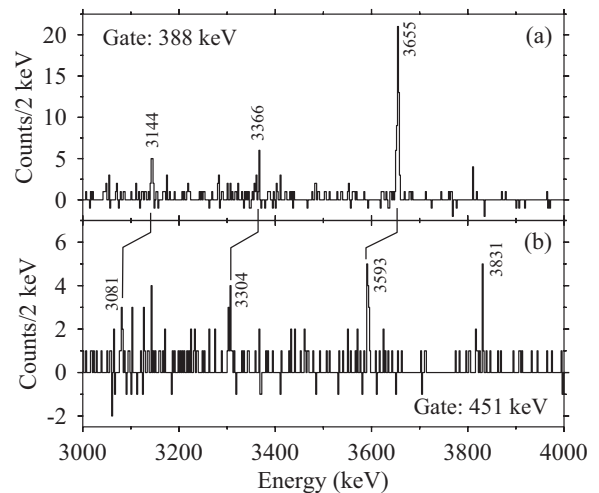


FIG. 3. Spectrum of  $\gamma$  rays observed in coincidence with (a) the 388 keV and (b) the 451 keV transition emitted after the first or second decay detected in WAS3ABi within 381 ms after the implantation of a  $^{130}\text{Cd}$  ion. In case (a) no prompt time gate was applied to account for the isomeric character of the 388 keV state.

further supported by the observation of a 2739 keV  $\gamma$  ray in coincidence with the 1016 keV but not the 1104 keV transition [see Fig. 2(c)]. In Ref. [8] a 2738 keV transition was placed to feed the 1669 keV state; however, no coincidence with the 1669 keV transition could be established in the present work.

To summarize the discussion up to this point, below the  $1^+$  state at 2120 keV we propose the existence of four excited states at energies of 388, 451, 950, and 1016 keV. This is in clear contrast to the excitation scheme presented in Refs. [5,8] in which, besides the known isomeric 388 keV state, levels at 1171 and 1669 keV have been established.

A closer inspection of Fig. 1 shows that, besides the  $\gamma$  rays discussed so far, a large number of additional lines are observed at energies above 3 MeV. Note that the energies of these lines do not agree with those of the high-energy transitions proposed in Ref. [8] (compare Table I). Only in the case of the 5393.3(5) keV  $\gamma$  ray observed in the present work, a correspondence to the 5391.0(10) keV line reported in that reference cannot be excluded. A closer look at the energies shows that there are several pairs of transitions whose energies differ by 63 keV, which corresponds to the energy difference between the 388 and 451 keV states. For several of these high-energy transitions coincidence relations with the 388 and 451 keV  $\gamma$  rays are observed, as illustrated in Fig. 3. Based on this information four new excited states at energies of 3532, 3717, 3755, and 4044 keV are unambiguously established. In some cases additional decay branches to the 950 and 1016 keV states are observed. The  $\gamma$  rays with 3967, 4066, and 4197 keV are not observed in coincidence with either the 388 or the 451 keV transition, although their intensities are comparable to the ones of the other high-energy transitions. These  $\gamma$  rays therefore have been tentatively assigned as populating the ground state (thin lines in Fig. 4). The 3967 keV  $\gamma$  ray is observed in coincidence with a 229 keV

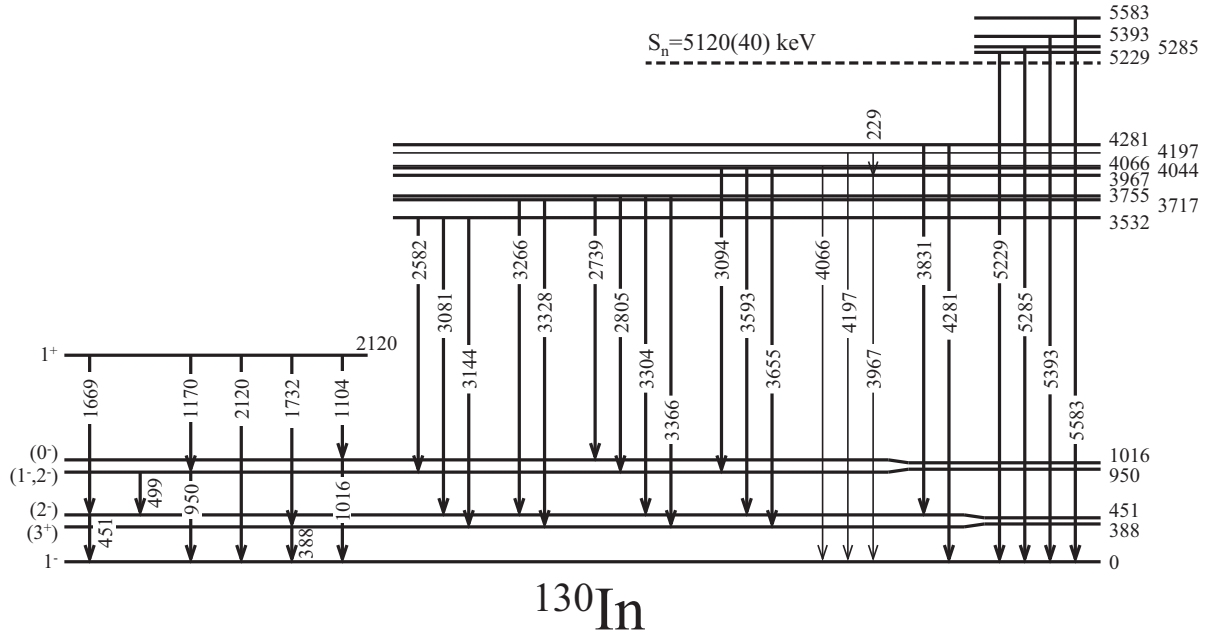


FIG. 4. Proposed level scheme of  $^{130}\text{In}$  established based on the coincidence relations between the  $\gamma$  rays emitted following the  $\beta$  decay of  $^{130}\text{Cd}$ . Tentatively placed  $\gamma$  rays are shown as thin lines.

transition which has tentatively been placed decaying from the 4197 keV state. Finally, the four  $\gamma$  rays with energies of 5229, 5285, 5393, and 5583 keV observed in Fig. 1 are assigned as ground state transitions, thus defining four new excited states positioned above the neutron separation energy of  $S_n = 5120(40)$  keV [18]. The reason for this assignment is that no coincidence relations could be established for these transitions, and furthermore the probability of observing  $\gamma$ -decaying excited states above the neutron separation energy is expected to decrease rapidly with increasing energy. Last, we would like to note that we observe a  $\gamma$  ray with an energy of 1314 keV (already reported in Ref. [8]), which seems to be emitted following the decay of  $^{130}\text{Cd}$  but cannot unequivocally be placed in the level scheme shown in Fig. 4 since no unique coincidence information is obtained. One possibility is that this transition directly populates the ground state.

The absolute intensity of the 451 keV transitions was determined to be 53.4(28) per 100 decays. With this value

and using the relative  $\gamma$ -ray intensities quoted in Table I, the  $\beta$  feeding to the individual excited states of  $^{130}\text{In}$  in the decay of the  $^{130}\text{Cd}$   $0^+$  ground state can be calculated based on the decay scheme presented in Fig. 4. The resulting  $\beta$  feeding as well as the corresponding  $\log ft$  values, calculated taking into account a half-life of  $T_{1/2} = 127(2)$  ms [3] and a  $\beta$ -decay energy of  $Q_\beta = 8350(160)$  keV [18], are listed in Table II. When calculating the direct feeding to the excited states, a significant imbalance was found for the 388 keV state. The sum of the intensities of the five transitions populating this state (1732, 3144, 3328, 3366, and 3655 keV) amounts to 150(15)% of the intensity of the 388 keV  $\gamma$  ray (see Table I). The reason for this is most probably an unobserved  $\gamma$  transition from the 388 keV,  $3^+$  to the  $\beta$  decaying ( $5^+$ ) state which is known to exist at an excitation energy 0–50 keV below the 388 keV level [19,20]. Note that in Ref. [20] an energy of 400(60) keV was reported for the ( $5^+$ ) state which we changed to 389(–50) keV since in order to decay via  $\beta$  decay this level must lie below the  $3^+$  state.

IV. DISCUSSION

In the preceding section a revised level scheme of  $^{130}\text{In}$  was established. In comparison to the scheme presented in Ref. [5] only the  $1^+$  state at 2120 keV was confirmed in the present work, while the levels at 1171, 1669, and 2586 keV were replaced by new excited states with energies of 451, 950, and 1016 keV. In the following this new excitation scheme will be compared to shell-model calculations which employ a two-body effective interaction derived from the CD-Bonn nucleon-nucleon potential renormalized by way of the  $V_{\text{low-}k}$  approach [21]. The interaction is constructed by assuming  $^{132}\text{Sn}$  as closed core and considering the full  $N = 50$ –82 major shell for neutrons (i.e., the  $0g_{7/2}, 1d_{5/2}, 1d_{3/2}, 2s_{1/2}$ , and

TABLE II. Excited states in  $^{130}\text{In}$  populated in the  $\beta$  decay of  $^{130}\text{Cd}$ , the observed  $\beta$ -feeding intensities, and the resulting  $\log ft$  values for each decay.

$E_x$ (keV)	$I_\beta$ (%)	$\log ft$	$E_x$ (keV)	$I_\beta$ (%)	$\log ft$
0			3967(2)	–0.2(2)	
388(1)			4044(2)	3.5(4)	4.6(1)
451(1)	–2(5)	>5.8	4066(2)	0.5(1)	5.4(1)
950(1)	0.5(14)	>5.9	4197(2)	1.3(2)	4.9(1)
1016(1)	2.2(5)	5.8(1)	4281(2)	0.4(1)	5.4(1)
2120(1)	74.2(67)	3.9(1)	5229(2)	0.4(1)	4.9(2)
3532(2)	1.1(2)	5.3(1)	5285(2)	0.6(1)	4.7(1)
3717(2)	0.3(2)	5.8(3)	5393(2)	0.4(1)	4.8(2)
3755(2)	1.7(3)	5.0(1)	5583(2)	0.1(1)	5.3(5)

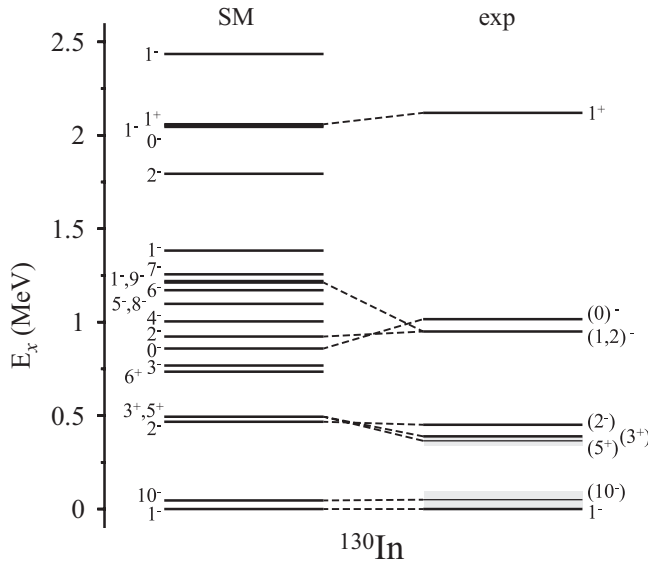


FIG. 5. Comparison of the low-energy part of the experimental level scheme of  $^{130}\text{In}$  with shell-model calculations (see text for details). The grey areas indicate the experimental uncertainties of the positions of the  $(10^-)$  and  $(5^+)$  states.

$0h_{11/2}$  orbitals) and the  $Z = 28-50$  shell for protons (i.e., the  $0f_{5/2}$ ,  $1p_{3/2}$ ,  $1p_{1/2}$ , and  $0g_{9/2}$  orbits). The  $\pi\pi$  pairing has been reduced to 88% and the  $\nu\nu$  and  $\pi\nu$  multipoles increased by factors of 1.6 and 1.5 in the dominant configurations  $\nu h_{11/2}^2$  and  $\nu h_{11/2}\pi g_{9/2}$ . The neutron single-particle energies were taken from Ref. [22], while for the protons energies of 0.365 ( $1p_{1/2}$ ) and 1.353 MeV ( $1p_{3/2}$ ) relative to the  $0g_{9/2}$  orbital as reported from very recent mass measurements and decay spectroscopy, respectively, were employed [23,24]. For the experimentally still unknown energy of the  $0f_{5/2}$  proton orbital a value of 2.6 MeV relative to  $0g_{9/2}$  was adopted to be consistent with the shell-model calculations presented in Refs. [24–27]. Effective charges  $e_\pi = 1.5e$  and  $e_\nu = 0.7e$  for  $E1$  and  $E2$ , and effective spin  $g$  factors  $g_s = 0.7g_s^{\text{free}}$  for  $M1$  transitions were used. Calculations were performed with the code OXBASH [28].

The results of the calculations for the excited states below 2.5 MeV are compared to experiment in Fig. 5. In contrast to the calculations presented in Ref. [7] the excitation energies of both  $\beta$ -decaying states, the  $(5^+)$  level at 388(–50) keV and the  $(10^-)$  state at 50(50) keV, as well as the  $(3^+)$  microsecond isomer, are well reproduced in the current approach. Also the calculated energy of 2059 keV for the  $\pi g_{9/2}^{-1}\nu g_{7/2}^{-1}$   $1^+$  state is very close to the experimental value of 2120 keV. Due to the inversion of the order within the 1669–451 keV cascade, the  $(1^-)$  state at 1669 keV reported previously was replaced in the current work by a level at an excitation energy of 451 keV. Based on the shell-model calculation we propose a spin of  $(2^-)$  for this state which is consistent with the observed feeding from the  $1^+$  state and the decay to the  $1^-$  ground state. Spins and parities of  $(0^-)$  and  $(1^-, 2^-)$  are tentatively assigned to the newly established states at excitation energies of 950 and 1016 keV, respectively. Note that the  $1^-$ ,  $10^-$ , and  $2^-$  states calculated at 0, 46, and 467 keV are members of the

$\pi g_{9/2}^{-1}\nu h_{11/2}^{-1}$  multiplet while the  $5^+$  and  $3^+$  levels both placed at 494 keV by the shell-model calculation are based on the  $\pi g_{9/2}^{-1}\nu d_{3/2}^{-1}$  configuration.

Taking the  $B(E2; 1^+ \rightarrow 3^+)$  value obtained in the NA-14 shell-model approach as a reference, estimates of the strengths of the  $E1$  transitions observed in the decay of the  $1^+$  state may be obtained based on the experimental branching ratios summarized in Table III. While for the 2120, 1104, and 1170 keV transitions  $B(E1)$  values in the range typical for  $E1$  strength in the  $^{132}\text{Sn}$  region are deduced, the strength of the 1699 keV  $\gamma$  ray is slightly larger but still compatible with the typical distribution. Note that these estimates of course depend on the reliability of the prediction for the  $E2$  transition used as reference. As can be read from Table III the branching ratios for the decay of the negative-parity states at 950 and 1016 keV are quite well reproduced by the present calculations, keeping in mind that retarded  $M1$  transitions are subject to uncertainties caused by small admixtures in the wave functions and effective operators used. Turning now to the decay of the  $(3^+)$  state at 388 keV we recall from the last section that the summed intensity of the  $\gamma$  rays populating this state is larger by about 50% as compared to the intensity of the depopulating 388 keV transition. This observation points to the existence of an unobserved  $E2$   $\gamma$ -decay branch to the  $\beta$ -decaying  $(5^+)$  level positioned 0–50 keV below the  $(3^+)$  state. The shell-model calculation clearly fails to reproduce the  $B(E2)$  value interval deduced from the lifetime of the  $(3^+)$  state and the experimental branching ratio assuming  $\gamma$ -ray energies in the range 20–50 keV (see Table III). Note, however, that the decay properties of this state are very sensitive to the unknown position of the  $0f_{5/2}$  proton orbital. Placing this orbital deep in the shell (6 MeV relative to  $0g_{9/2}$ ), agreement within a factor of 2 to 3 is found.

All states established at excitation energies above 3.5 MeV (see Fig. 4) most likely contain core-excited configurations based on the excitation of either a neutron from an orbital below  $N = 82$  to one above or a proton across  $Z = 50$ . Such core-excited states have been established in doubly-magic  $^{132}\text{Sn}$  as well as in all of its direct neighbors except for the two most exotic, namely  $^{133}\text{Sn}$  and  $^{132}\text{In}$ . In  $^{132}\text{Sn}$  excited states with the neutron configurations  $\nu(f_{7/2}h_{11/2}^{-1})$ ,  $\nu(f_{7/2}d_{3/2}^{-1})$ , and  $\nu(f_{7/2}g_{7/2}^{-1})$  were identified at excitation energies around 4.7, 4.8, and 7.2 MeV, respectively, while the lowest core-excited proton configuration  $\pi(g_{7/2}g_{9/2}^{-1})$  was identified around 5.5 MeV [29,30]. The  $\nu(f_{7/2}h_{11/2}^{-1})$  and  $\nu(f_{7/2}g_{7/2}^{-1})$  states coupled to a  $g_{9/2}$  proton hole have recently also been observed in  $^{131}\text{In}$  at slightly shifted excitation energies of 4.0 and 5.8 MeV [27]. In  $^{131}\text{Sn}$  and  $^{132}\text{Sb}$  the  $\nu(f_{7/2}h_{11/2}^{-1})$  and  $\nu(f_{7/2}d_{3/2}^{-1})$  neutron excitations coupled to a  $h_{11/2}$  neutron hole respectively, a  $h_{11/2}$  neutron hole and a  $g_{7/2}$  proton were identified in overlapping energy ranges between 4 and 5 MeV [31,32]. In the present case of  $^{130}\text{In}$ , the existence of negative-parity four-quasiparticle (4qp) states with configuration  $\pi g_{9/2}^{-1}\nu(f_{7/2}h_{11/2}^{-2})$  as well as positive-parity 4qp states with  $\pi g_{9/2}^{-1}\nu(f_{7/2}h_{11/2}^{-1}d_{3/2}^{-1})$  and  $\pi g_{9/2}^{-1}\nu(f_{7/2}h_{11/2}^{-1}g_{7/2}^{-1})$  configuration can therefore be anticipated. The states belonging to the first two configurations are expected to be rather close in

TABLE III. Transition strengths and branching ratios for the  $\gamma$  rays observed in the decay of the  $1^+$  state at an excitation energy of 2120 keV in  $^{130}\text{In}$ . All transition strengths are obtained using the theoretical  $B(E2; 1^+ \rightarrow 3^+)$  value as reference.

$I_i^\pi$	$I_f^\pi$	$E_\gamma$ (keV)	$\sigma L$	Experimental		Shell model	
				$b$ (%)	$B(\sigma L)$ (W.u.)	$b$ (%)	$B(\sigma L)$ (W.u.)
$1^+$	$3^+$	1732	$E2$	4(1)	ref.		0.9381
	$1_1^-$	2120	$E1$	8(1)	$6.4 \times 10^{-5}$		
	$2_1^-$	1669	$E1$	72(9)	$1.1 \times 10^{-3}$		
	$0_1^-$	1104	$E1$	1(1)	$7.8 \times 10^{-5}$		
	$2_2^-$	1170 <sup>a</sup>	$E1$	15(2)	$6.9 \times 10^{-4}$		
$0^-$	$1_2^-$	1170 <sup>a</sup>	$E1$	15(2)			
	$2_1^-$	565	$E2$	<12		<0.001	0.006
$2_2^-$	$1_1^-$	1016	$M1$	100(12)		100	0.101
	$2_1^-$	499 <sup>a</sup>	$M1$	6(1)		32.3	0.037
			$E2$				0.110
$1_2^-$	$1_1^-$	950 <sup>a</sup>	$M1$	94(1)		67.7	0.106
			$E2$				0.004
	$2_1^-$	499 <sup>a</sup>	$M1$	6(1)		13.4	0.012
$3^+$			$E2$				0.641
	$1_1^-$	950 <sup>a</sup>	$M1$	94(1)		86.6	0.111
			$E2$				0.092
$3^+$	$5^+$	50 <sup>b</sup>	$E2$	33(7)	0.18(4)		1.618 <sup>c</sup>
		20 <sup>b</sup>	$E2$		0.42(8)		1.304 <sup>d</sup>
	$1_1^-$	388	$M2$	67(7)	0.020(2)		0.196 <sup>c</sup>
							0.041 <sup>d</sup>

<sup>a</sup>Alternative assignments.

<sup>b</sup>Alternative  $E_\gamma$ , including conversion.

<sup>c</sup> $E_x(0f_{5/2}) = 2.57$  MeV.

<sup>d</sup> $E_x(0f_{5/2}) = 5.87$  MeV.

energy while the latter should have slightly higher excitation energy in agreement with the findings in  $^{132}\text{Sn}$ ,  $^{131}\text{Sn}$ , and  $^{131}\text{In}$ . We therefore tentatively assign a spin of  $1^+$  and the configuration  $\pi g_{9/2}^{-1}\nu(f_{7/2}h_{11/2}^{-1}g_{7/2}^{-1})$  to the newly established states above 5 MeV. Their neutron decay to the  $^{129}\text{In}$  ground state is hindered as it requires  $\ell = 4$ . The states in the energy range 3.5–4.3 MeV may be of either  $\pi g_{9/2}^{-1}\nu(f_{7/2}h_{11/2}^{-2})$  or  $\pi g_{9/2}^{-1}\nu(f_{7/2}h_{11/2}^{-1}d_{3/2}^{-1})$  configuration; no clear assignment can be made on the basis of the  $\log ft$  values presented in Table II. However, the states at 3532, 3717, 3755, and 4044 keV more likely have spin  $1^+$  and the  $\pi g_{9/2}^{-1}\nu(f_{7/2}h_{11/2}^{-1}d_{3/2}^{-1})$  configuration because they decay to both the 388 keV, ( $3^+$ ) and 451 keV, ( $2^-$ ) levels which belong to the  $\pi g_{9/2}^{-1}\nu d_{3/2}^{-1}$  and  $\pi g_{9/2}^{-1}\nu h_{11/2}^{-1}$  multiplets, respectively. On the other hand the 3967, 4066, 4197, and 4281 keV levels, for which no decay branches to the ( $3^+$ ) state could be established, may be based on the negative-parity  $\pi g_{9/2}^{-1}\nu(f_{7/2}h_{11/2}^{-2})$  configuration. Clearly additional information is required in order to fix the structure of all states with excitation energies above 3.5 MeV.

### V. CONCLUSIONS

The  $\beta$  decay of the  $N = 82$  nucleus  $^{130}\text{Cd}$  was studied at the RIBF facility at the RIKEN Nishina Center. The clean ion identification and the high  $\gamma$ -ray detection efficiency of the present experiment enabled a thorough examination, based

on  $\gamma$ - $\gamma$  coincidence information, of the excitation scheme of  $^{130}\text{In}$  published prior to this work [5]. While the energy of the first excited  $1^+$  state at 2120 keV was confirmed, the excited states proposed in Ref. [5] at 1171, 1669, and 2586 keV were replaced in the present work by new levels at 451, 950, and 1016 keV. Furthermore, the decays of twelve excited states in the energy intervals 3.5–4.3 and 5.2–5.6 MeV were observed, four of them positioned above the neutron separation energy. The low-energy part of the excitation scheme was compared to shell-model calculations and a good agreement was found. Core-excited configurations are tentatively proposed for the states above 3.5 MeV. However, further investigations are needed in order to fix the structure of these states.

### ACKNOWLEDGMENTS

We thank the staff of the RIKEN Nishina Center accelerator complex for providing stable beams with high intensities to the experiment. We acknowledge the EUROBALL Owners Committee for the loan of germanium detectors and the PreSpec Collaboration for the readout electronics of the cluster detectors. This work was supported by the Spanish Ministerio de Ciencia e Innovaci3n under contract FPA2011-29854-C04 and the Spanish Ministerio de Econom3a y Competitividad under Contract No. FPA2014-57196-C5-4-P, the Generalitat Valenciana (Spain) under Grant No.

PROMETEO/2010/101, the National Research Foundation of Korea (NRF) grant funded by the Korea government (MEST) (NRF-2014S1A2A2028636, 2016K1A3A7A09005579), the Priority Centers Research Program in Korea (2009-0093817), OTKA Contract No. K-100835, JSPS KAKENHI (Grant No. 25247045), the European Commission through the Marie Curie Actions call FP7-PEOPLE-2011-IEF under Contract

No. 300096, the US Department of Energy, Office of Nuclear Physics, under Contract No. DE-AC02-06CH11357, the STFC (UK), the “RIKEN foreign research program,” the German BMBF (No. 05P12RDCIA, No. 05P12RDNUP, and No. 05P12PKFNE), HIC for FAIR, the DFG cluster of excellence “Origin and Structure of the Universe,” and DFG (Contract No. KR2326/2-1).

- 
- [1] K.-L. Kratz, H. Gabelmann, W. Hillebrandt, B. Pfeiffer, K. Schlösser, and F.-K. Thielemann, *Z. Phys. A* **325**, 489 (1986).
- [2] M. Hannawald *et al.*, *Nucl. Phys. A* **688**, 578 (2001).
- [3] G. Lorusso *et al.*, *Phys. Rev. Lett.* **114**, 192501 (2015)
- [4] R. Dunlop *et al.*, *Phys. Rev. C* **93**, 062801(R) (2016).
- [5] I. Dillmann, K. L. Kratz, A. Wöhr, O. Arndt, B. A. Brown, P. Hoff, M. Hjorth-Jensen, U. Koster, A. N. Ostrowski, B. Pfeiffer, D. Seweryniak, J. Shergur, and W. B. Walters, *Phys. Rev. Lett.* **91**, 162503 (2003).
- [6] G. Martínez-Pinedo and K. Langanke, *Phys. Rev. Lett.* **83**, 4502 (1999).
- [7] J. J. Cuenca-García, G. Martínez-Pinedo, K. Langanke, F. Nowacki, and I. N. Borzov, *Eur. Phys. J. A* **34**, 99 (2007).
- [8] <http://www.nndc.bnl.gov/ensdf/>, full evaluation of data for  $^{130}\text{In}$  by Balraj Singh, ENSDF, 31 May 2008.
- [9] S. Nishimura, *Prog. Theor. Exp. Phys.* (2012) 03C006; S. Nishimura *et al.*, RIKEN Accel. Progr. Rep. **46**, 182 (2013).
- [10] P.-A. Söderström *et al.*, *Nucl. Instrum. Methods B* **317**, 649 (2013).
- [11] T. Kubo *et al.*, *Prog. Theor. Exp. Phys.* (2012) 03C003.
- [12] N. Fukuda *et al.*, *Nucl. Instrum. Methods B* **317**, 323 (2013).
- [13] J. Eberth *et al.*, *Nucl. Instrum. Methods Phys. Res., Sect. A* **369**, 135 (1996).
- [14] J. Simpson, *Z. Phys. A* **358**, 139 (1997).
- [15] B. Fogelberg, K. Heyde, and J. Sau, *Nucl. Phys. A* **352**, 157 (1981).
- [16] M. Hellström *et al.*, in *Nuclear Structure and Dynamics at the Limits: Proceedings of the International Workshop XXXI on Gross Properties of Nuclei and Nuclear Excitations*, Hirscheegg, Austria, 2003, edited by H. Feldmeier (Gesellschaft für Schwerionenforschung (GSI), Darmstadt, 2003), p. 72.
- [17] A. Scherillo, J. Genevey, J. A. Pinston, A. Covello, H. Faust, A. Gargano, R. Orlandi, G. S. Simpson, I. Tsekhanovich, and N. Warr, *Phys. Rev. C* **70**, 054318 (2004).
- [18] M. Wang *et al.*, *Chin. Phys. C* **36**, 1603 (2012).
- [19] B. Fogelberg, A. Aprahamian, R. L. Gill, H. Mach, and D. Rehfield, *Phys. Rev. C* **31**, 1026 (1985).
- [20] L. Spanier *et al.*, *Nucl. Phys. A* **474**, 359 (1987).
- [21] L. Coraggio *et al.*, *Prog. Part. Nucl. Phys.* **62**, 135 (2009).
- [22] H. Grawe, K. Langanke, and G. Martínez-Pinedo, *Rep. Prog. Phys.* **70**, 1525 (2007).
- [23] A. Kankainen, J. Hakala, T. Eronen, D. Gorelov, A. Jokinen, V. S. Kolhinen, I. D. Moore, H. Penttilä, S. Rinta-Anttila, J. Rissanen, A. Saastamoinen, V. Sonnenschein, and J. Aysto, *Phys. Rev. C* **87**, 024307 (2013).
- [24] J. Taprogge *et al.*, *Phys. Rev. Lett.* **112**, 132501 (2014).
- [25] J. Taprogge *et al.*, *Phys. Rev. C* **91**, 054324 (2015)
- [26] J. Taprogge *et al.*, *Phys. Lett. B* **738**, 223 (2014).
- [27] J. Taprogge *et al.*, *Eur. Phys. J. A* (to be published).
- [28] B. A. Brown *et al.*, OXBASH for windows, MSU-NSCL Report 1289, 2004 (unpublished).
- [29] B. Fogelberg, M. Hellström, D. Jerrestam, H. Mach, J. Blomqvist, A. Kerek, L. O. Norlin, and J. P. Omtvedt, *Phys. Rev. Lett.* **73**, 2413 (1994).
- [30] T. Björnstad *et al.*, *Nucl. Phys. A* **453**, 463 (1986).
- [31] P. Bhattacharyya, P. J. Daly, C. T. Zhang, Z. W. Grabowski, S. K. Saha, R. Broda, B. Fornal, I. Ahmad, D. Seweryniak, I. Wiedenhover, M. P. Carpenter, R. V. F. Janssens, T. L. Khoo, T. Lauritsen, C. J. Lister, P. Reiter, and J. Blomqvist, *Phys. Rev. Lett.* **87**, 062502 (2001).
- [32] P. Bhattacharyya, P. J. Daly, C. T. Zhang, Z. W. Grabowski, S. K. Saha, B. Fornal, R. Broda, W. Urban, I. Ahmad, D. Seweryniak, I. Wiedenhover, M. P. Carpenter, R. V. F. Janssens, T. L. Khoo, T. Lauritsen, C. J. Lister, P. Reiter, and J. Blomqvist, *Phys. Rev. C* **64**, 054312 (2001).